Mechanism of Action of *Escherichia coli* Phosphoribosylaminoimidazolesuccinocarboxamide Synthetase[†]

Scott W. Nelson,[‡,§] Daniel J. Binkowski,[§] Richard B. Honzatko, and Herbert J. Fromm*

Department of Biochemistry, Biophysics, and Molecular Biology, Iowa State University, Ames, Iowa 50011

Received August 20, 2004; Revised Manuscript Received October 27, 2004

ABSTRACT: The conversion of ATP, L-aspartate, and 5-aminoimidazole-4-carboxyribonucleotide (CAIR) to 5-aminoimidazole-4-(*N*-succinylcarboxamide) ribonucleotide (SAICAR), ADP, and phosphate by phosphoribosylaminoimidazolesuccinocarboxamide synthetase (SAICAR synthetase) represents the eighth step of de novo purine nucleotide biosynthesis. SAICAR synthetase and other enzymes of purine biosynthesis are targets of natural products that impair cell growth. Prior to this study, no kinetic mechanism was known for any SAICAR synthetase. Here, a rapid equilibrium random ter-ter kinetic mechanism is established for the synthetase from *Escherichia coli* by initial velocity kinetics and patterns of linear inhibition by IMP, adenosine 5′-(β,γ-imido)triphosphate (AMP-PNP), and maleate. Substrates exhibit mutual binding antagonism, with the strongest antagonism between CAIR and either ATP or L-aspartate. CAIR binds to the free enzyme up to 200-fold more tightly than to the ternary enzyme−ATP−aspartate complex, but the latter complex may be the dominant form of SAICAR synthetase in vivo. IMP is a competitive inhibitor with respect to CAIR, suggesting the possibility of a hydrogen bond interaction between the 4-carboxyl and 5-amino groups of enzyme-bound CAIR. Of several aspartate analogues tested (hadacidin, L-malate, succinate, fumarate, and maleate), maleate was by far the best inhibitor, competitive with respect to L-aspartate. Inhibition by IMP and maleate is consistent with a chemical mechanism for SAICAR synthetase that parallels that of adenylosuccinate synthetase.

Phosphoribosylaminoimidazolesuccinocarboxamide synthetase [EC 6.3.2.6, 5′-phosphoribosyl-4-carboxy-5-aminoimidazole:L-aspartate ligase (ADP)] (SAICAR synthetase)[1] catalyzes the eighth step in de novo purine nucleotide biosynthesis:

ATP + L-aspartate + 5-aminoimidazole-4-carboxyribonucleotide (CAIR) → 5-aminoimidazole-4-(*N*-succinylcarboxamide) ribonucleotide (SAICAR) + ADP + P_i

Lukens and Buchanan (*1*) first described the enzyme in 1959, and in 1962, Miller and Buchanan (*2*) demonstrated its presence in a variety of life forms and reported the purification and properties of the synthetase from chicken liver. More recently, the Stubbe laboratory purified SAICAR synthetase from *Escherichia coli* (*3*).

Our laboratory has investigated bacterial and mammalian adenylosuccinate synthetases (AMPSase) since 1958 (*4*−*7*). The substrates for AMPSase and SAICAR synthetase are identical or similar: GTP, IMP, and ASP for AMPSase correspond to ATP, CAIR, and ASP for SAICAR synthetase. In addition, the two reaction products, SAICAR and adenylosuccinate, are each substrates for adenylosuccinate lyase. AMPSase and SAICAR synthetase from *E. coli*, however, exhibit only 16% sequence identity. SAICAR synthetase from *E. coli* is a trimer (*3*) and from *Saccharomyces cerevisiae* a monomer (*11*), whereas all well-characterized AMPSases are functional dimers (*12*−*16*). Mammalian SAICAR synthetase is a bifunctional enzyme, combining 5-aminoimidazole ribonucleotide carboxylase (AIR carboxylase) and SAICAR synthetase activities (*2*), whereas *E. coli* and *S. cerevisiae* SAICAR synthetases have no carboxylase activity.

L-Alanosine can replace ASP as a substrate in vivo for SAICAR synthetase and in vitro for AMPSase (*8*−*10*). The product of the SAICAR synthetase reaction, L-alanosyl-5-amino-4-imidazolecarboxylic acid ribonucleotide, is a potent inhibitor of AMPSase and adenylosuccinate lyase, being the compound responsible for L-alanosine toxicity (*9*). Many cancers (approximately 30% of all T-cell acute lymphocytic leukemia, for instance) lack a salvage pathway for adenine nucleotides and rely entirely on adenylosuccinate synthetase and de novo biosynthesis (*17*). L-Alanosine is toxic to cell lines of such cancers at concentrations well below those that poison cells with intact salvage pathways. Hence, L-alanosine may be effective as a chemotherapeutic agent in combination with other drugs (*17*). Efforts to further develop specific inhibitors of de novo purine biosynthesis would benefit from

[†] This work was supported by National Institutes of Health Research Grant NS 10546.

* Corresponding author. Telephone: (515) 294-4971. Fax: (515) 294-0453. E-mail: hjfromm@iastate.edu.

[‡] Current address: Department of Chemistry, The Pennsylvania State University, University Park, PA 16802.

[§] These authors contributed equally to this work.

[1] Abbreviations: SAICAR synthetase, phosphoribosylaminoimidazolesuccinocarboxamide synthetase; AMPSase, adenylosuccinate synthetase; ASP, L-aspartate; CAIR, 5-aminoimidazole-4-carboxyribonucleotide; SAICAR, 5-aminoimidazole-4-(*N*-succinylcarboxamide) ribonucleotide; AMP-PNP, adenosine 5′-(β,γ-imido)triphosphate; CAIRs, 5-aminoimidazole-4-carboxyribonucleoside; AICARs, 5-aminoimidazole-4-carboxamide ribonucleoside.

10.1021/bi048191w CCC: $30.25
Published on Web 12/18/2004

a basic understanding of structure−functions relations in enzymes participating in purine biosynthesis, and for SAICAR synthetase such information is lacking.

We have undertaken studies on *E. coli* SAICAR synthetase to determine whether further parallels exist between it and AMPSase with respect to substrate recognition and possible reaction mechanisms. Initial velocity kinetics of SAICAR synthetase, using competitive inhibitors of ATP, CAIR, and ASP, are consistent with a rapid equilibrium sequential mechanism, in which substrates add randomly to the active site, a kinetic mechanism comparable to that of AMPSase (*18*, *19*). The efficacy of maleate (but not fumarate) as a competitive inhibitor of SAICAR synthetase with respect to ASP suggests a *cis*-like conformation from the amino acid substrate in its enzyme-bound state, and indeed, ligated crystal structures of AMPSase indicate a *cis*-like conformation for ASP (*20*). On the other hand, the absence of inhibition of SAICAR synthetase by hadacidin, and its potent inhibition of AMPSase, suggests fundamental differences in the recognition of the α-amino group of ASP by the two enzymes. IMP is a competitive inhibitor of SAICAR synthetase with respect to CAIR, consistent with the formation of a purine-like hydrogen-bonded ring between the 4-carboxylate and 5-amino groups of CAIR. Finally, mechanisms of catalysis of AMPSase and SAICAR synthetase may exhibit significant parallels, such as the use of a single side chain as a catalytic base in the formation of the carbonyl phosphate intermediate.

EXPERIMENTAL PROCEDURES

Materials. ATP, adenosine 5′-(β,γ-imido)triphosphate (AMP-PNP), IMP, ASP, L-malate, maleate, fumarate, NADH, phosphoenolpyruvate, pyruvate kinase, and lactate dehydrogenase were purchased from Sigma. 5-Aminoimidazole-4-carboxamide ribonucleoside (AICARs) was purchased from Toronto Research Biochemicals. L-Alanosine was obtained from the Drug Research and Development Branch, National Cancer Institute, Bethesda, MD. Ampli-Taq DNA polymerase was purchased from Midwest Scientific. Restriction enzymes were purchased from New England Biolabs. *E. coli* strains XL1-Blue and BL21(DE3) came from Stratagene and Invitrogen, respectively. Hadacidin was a gift from Drs. Bruce Cooper and Fred Rudolph, Department of Biochemistry and Cell Biology, Rice University.

PurC Cloning and SAICAR Synthetase Purification. Genomic DNA was isolated from *E. coli* strain XL1-Blue using the Promega genomic DNA purification kit. The open reading frame encoding SAICAR synthetase was PCR amplified using the following forward and reverse primers, respectively: 5′-GCTAGCATATGCAAAAGCAAGCTGAG-3′ and 5′-CCGCTCGAGTCAGTCCAGCTGTACACC-3′. The underlined sequences indicate *Nde*I and *Xho*I restriction sites, respectively, which were used to clone the PCR product into the pet24b vector. The pet24b expression vector, containing wild-type PurC, was transformed into BL21(DE3) *E. coli*, and a single colony was used to inoculate a 100 mL overnight culture of Luria broth. Six liters of Luria broth in 12 flasks was inoculated with 5 mL of overnight culture each and grown to an absorbance of 1.0 at 600 nm. The cells were then cooled to 16 °C, induced with 0.25 mM IPTG, and allowed to grow an additional 16 h before being harvested by centrifugation. Purification of native SAICAR synthetase was performed as described by Meyer et al. (*3*).

The conventional purification of SAICAR synthetase requires several steps and, in our hands at least, resulted in a protein with a tendency toward aggregation. As an alternative, we incorporated an N-terminal, hexahistidine tag and employed nickel nitrilotriacetic acid−agarose chromatography. The wild-type PurC gene was subcloned into the pet100/TOPO vector (Invitrogen) using the forward primer 5′-CACCTCAAATGAAGTTGAACAG-3′ and a reverse primer identical to that used in the pet24b cloning. Hexahistidine-tagged enzyme was expressed as described above for the native enzyme. The harvested cell pellet was suspended in 80 mL of 20 mM KP_i, 500 mM NaCl, and 10 mM imidazole (pH 8.0) and lysed using a French press at 20000 psi. After centrifugation at 15000*g* for 45 min, the cell-free extract was loaded onto a nickel nitrilotriacetic acid−agarose column and washed with 10 column volumes of lysis buffer. A second wash was performed with 10 column volumes of lysis buffer containing 40 mM imidazole. Lysis buffer containing 250 mM imidazole eluted SAICAR synthetase from the column. Protein purity and concentration were confirmed by SDS−polyacrylamide gel electrophoresis (*21*) and by Bradford assay (*22*), respectively.

Synthesis of CAIR. 5-Aminoimidazole-4-carboxyribonucleoside (CAIRs) was synthesized from 5-aminoimidazole-4-carboxamide ribonucleoside (AICARs) under alkaline conditions as described by Srivastava et al. (*23*) with minor modifications as follows: 0.516 g of AICARs was purged with N_2 gas for 10 min prior to addition of 2 mL of freshly prepared 6 M NaOH. The reaction mixture was refluxed gently for 4 h under N_2 gas and then cooled to 0 °C. Four milliliters of ethanol was added to the cooled mixture. The resulting thick syrup was triturated six times with 1 mL of ethanol and lyophilized overnight. The dry glassy solid from lyophilization was triturated once with 0.5 mL of methanol and dried in a Speed-Vac. CAIRs was then resuspended in 500 mL of 5 mM NH_4HCO_3 and applied to a DEAE-Sephadex column equilibrated with 5 mM NH_4HCO_3. The column was washed with 10 volumes of 20 mM NH_4HCO_3 before eluting pure CAIRs with 150 mM NH_4HCO_3. The product was lyophilized to dryness overnight to remove volatile salts.

CAIRs was phosphorylated to CAIR using the procedure described by Meyer et al. (*3*), which is a modification of the method of Yoskikawa et al. (*24*). CAIR was purified using a DEAE-Sephadex column with a linear gradient of 50−400 mM NH_4HCO_3. Phosphate content was determined using alkaline phosphatase to hydrolyze the phosphate from CAIR. The amount of released inorganic phosphate was determined by the ammonium molybdate assay (*25*).

Size-Exclusion HPLC. Determination of the oligomeric state of hexahistidine-tagged SAICAR synthetase employed a Tsk-gel Super SW 3000 column from Tosoh Bioscience and an eluent buffer composed of 50 mM Hepes, pH 7.8, 200 mM KCl, 6 mM $MgCl_2$, and 1 mM dithiothreitol (DTT). The following standard proteins were injected (total volume 0.1 mL) as a mixture in which each had a concentration of approximately 2 mg/mL: cytochrome *c* (12.4 kDa), bovine serum albumin (66 kDa), aldehyde dehydrogenase (150 kDa), and β-amylase (200 kDa). SAICAR synthetase (2 mg/mL) was combined with the standard proteins, injected onto the

column, and run under conditions identical to those of the standard proteins.

Kinetic Experiments. All enzyme assays were carried out at 37 °C. Hydrolysis of ATP was monitored at 340 nm using pyruvate kinase and lactate dehydrogenase to couple the phosphorylation of ADP by phosphoenolpyruvate to the oxidation of NADH to NAD^+. The buffer conditions used in the assay were as follows: 50 mM Hepes, 20 mM KCl, 6 mM $MgCl_2$, 0.2 mM NADH, 2 mM phosphoenolpyruvate, 10 units of pyruvate kinase, and 5 units of lactate dehydrogenase, pH 7.8. Generally, 1 μg of SAICAR synthetase was used in an assay volume of 1.0 mL. The validity of the coupled assay was affirmed by a linear relationship, starting at the origin, in plots of velocity versus enzyme concentration. Experiments without inhibitor held one of three substrates at a saturating concentration, while varying the concentrations of the other two substrates systematically about their respective K_m values. Inhibition experiments held two of three substrate concentrations at twice their respective K_m values, while varying the concentration of the third substrate. Concentrations of substrates in specific assays appear in the figure legends. Kinetic data were fitted using a MINITAB program with an α value of 2.0 (*26*, *27*). The most appropriate models of inhibition were selected on the basis of *F*-tests and "goodness of fit" analysis.

RESULTS

PurC Cloning and SAICAR Synthetase Purification. Purification of the native enzyme requires three chromatographic steps and several days. The introduction of the hexahistidine tag to the N-terminus of SAICAR synthetase facilitates the purification of large quantities of active enzyme. Enzyme of at least 95% purity results directly from nickel nitrilotriacetic acid−agarose chromotography as determined by SDS−polyacrylamide gel electrophoresis (data not shown).

Synthesis of CAIR. We initially attempted the phosphorylation of CAIRs, using bovine liver adenosine kinase (*28*). Unfortunately, our preparation of partially purified adenosine kinase efficiently phosphorylated adenosine and AICARs but not CAIRs (data not shown). Chemical phosphorylation of CAIR was complete and selective, giving a purified product with 1 mole equiv of phosphate (data not shown). The absorbance spectrum of CAIR was identical to that of Lukens and Buchanan (*29*). Purified CAIR supported SAICAR synthetase activity, and the product of that reaction behaved identically to SAICAR in anion-exchange and reverse-phase chromatography. The overall yield of CAIR from AICARs was approximately 30%.

Size Exclusion HPLC Chromatography. Data from size exclusion chromatography (not shown) indicate a mass of approximately 87 kDa for hexahistidine-tagged SAICAR synthetase. The calculated subunit molecular mass of the hexahistidine-tagged enzyme (30.827 kDa) suggests a trimeric subunit assembly for the native protein. This finding agrees with data from analytical ultracentrifugation of the native enzyme (*3*) and indicates little or no disruption of the native structure due to the addition of the N-terminal hexahistidine tag.

Enzymatic Properties. The K_m values for CAIR, ASP, and ATP for native SAICAR synthetase are comparable to the corresponding values of Table 1 (K_a, K_b, and K_c) for the hexahistidine-tagged enzyme. The K_m for CAIR is more than 5-fold lower than that reported by Meyer et al. (*3*). The reason for the difference is unclear; however, CAIR is unstable even when stored as a dry solid at −20 °C, and this may account for the descrepancy in K_m values. The K_m for CAIR for yeast SAICAR synthetase (1.6 μM) is comparable to what we find for the *E. coli* enzyme (*10*). The K_m for L-alanosine is 0.9 mM.

Table 1: Rapid Equilibrium Random Sequential Model for SAICAR Synthetase[a]

equilibrium	parameter	fitted values and weighted mean
	specific activity	21 ± 1 (Figure 1a) 19 ± 1 (Figure 1b) 17.9 ± 0.8 (Figure 1c) 18.7 ± 0.6 (mean)
EABC = EBC + A	K_a	7.9 ± 0.6 (Figure 1a) 5.9 ± 0.4 (Figure 1b) 6.6 ± 0.3 (mean)
EABC = EAC + B	K_b	63 ± 5 (Figure 1a) 59 ± 4 (Figure 1c) 60 ± 3 (mean)
EABC = EAB + C	K_c	850 ± 80 (Figure 1b) 770 ± 50 (Figure 1c) 790 ± 40 (mean)
EBC = EC + B	K_{bc}	4 ± 1 (Figure 1a)
EAB = EB + A	K_{ab}	0.5 ± 0.1 (Figure 1b)
EAC = EA + C	K_{ca}	200 ± 30 (Figure 1c)
EAC = EC + A	$K_{ac} = K_{bc}K_a/K_b$	0.5 ± 0.2
EBC = EB + C	$K_{cb} = K_{ab}K_c/K_a$	70 ± 20
EAB = EA + B	$K_{ba} = K_{ca}K_b/K_c$	15 ± 2
EA = E + A	$K_{ia} = K_{ab}/\gamma$	0.04 ± 0.01
	$K_{ia} = K_{ac}/\beta$	0.05 ± 0.02 0.04 ± 0.01 (mean)
EB = E + B	$K_{ib} = K_{bc}/\alpha$	1.0 ± 0.4
	$K_{ib} = K_{ba}/\gamma$	1.1 ± 0.4 1.0 ± 0.3 (mean)
EC = E + C	$K_{ic} = K_{ca}/\beta$	19 ± 6
	$K_{ic} = K_{cb}/\alpha$	17 ± 6 18 ± 4 (mean)
	$\gamma = K_b/K_{bc} = K_a/K_{ac}$	15 ± 5
	$\beta = K_a/K_{ab} = K_c/K_{cb}$	11 ± 3
	$\alpha = K_c/K_{ca} = K_b/K_{ba}$	3.9 ± 0.7

[a] The symbol E represents hexahistidine-tagged SAICAR synthetase, and substrates A, B, and C represent CAIR, ATP, and ASP, respectively. Indicated parenthetically are the data used in determining the fitted value for a parameter. The model has seven independent parameters (the first entries listed) with all other parameters dependent on the first seven as indicated. The weighted mean is $\sum(1/\sigma_j)^2P_j/\sum(1/\sigma_j)^2$, where the summations run over independent determinations of a specific parameter, P_j, and its standard deviation, σ_j. Values for equilibrium constants are μM. Parameters α, β, and γ are ratios of equilibrium constants indicated in the table. All calculations employed six-digit values, the final entry being rounded to its first significant digit.

Metal Ion Specificity of SAICAR Synthetase. Concentrations of Mg^{2+} (1−10 mM) and Mn^{2+} (1−10 mM) have no significant effect on the capacity of the coupling assay to convert ADP into NAD^+. Hence, the coupled assay reflects the kinetics of SAICAR synthetase over the range of concentrations of Mg^{2+} and Mn^{2+} used here. The maximum velocity for the Mn^{2+}-activated enzyme is 50% of that for the Mg^{2+}-activated enzyme. Using saturating substrate levels ($5K_m$), optimal velocities occurred at 6 and 7 mM Mg^{2+} and Mn^{2+}, respectively. As Ca^{2+} did not support the activity of the coupling assay, the formation of SAICAR was monitored directly by absorbance changes at 290 nm. Ca^{2+} did not support catalysis in the presence of saturating concentrations

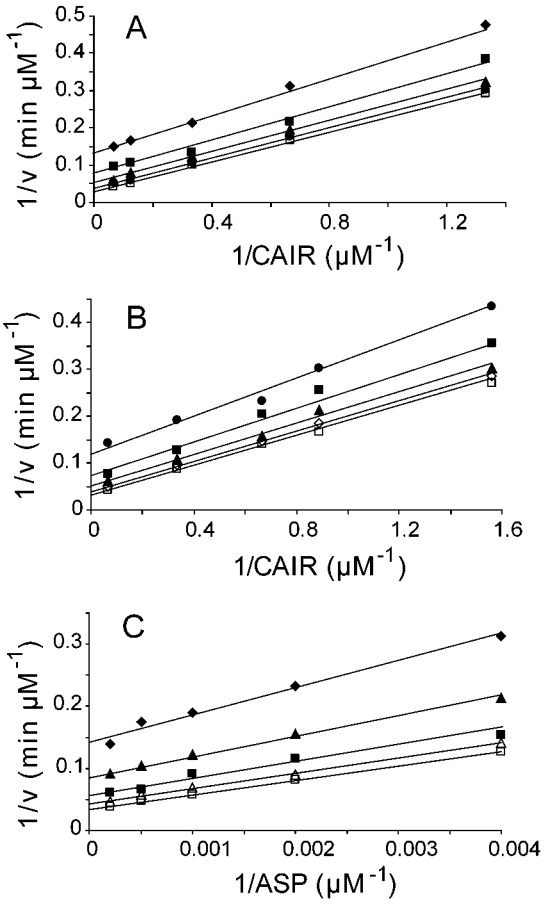

FIGURE 1: Plots of reciprocal velocity versus reciprocal substrate concentration. Mg^{2+} and ATP were added in a ratio of 1:1 to a solution containing 50 mM Hepes, 20 mM KCl, 6 mM $MgCl_2$, 0.2 mM NADH, 2 mM PEP, 10 units of pyruvate kinase, and 5 units of lactate dehydrogenase, pH 7.8. Lines come from eqs 2a−c using the parameters of Table 1. (A) CAIR was varied from 0.75 to 15 μM at fixed ATP concentrations of 15 (◆), 30 (■), 60 (▲), 120 (●), and 300 (□) μM. The concentration of ASP was 10 mM in each assay. (B) CAIR was varied from 0.64 to 15 μM at fixed ASP concentrations of 250 (●), 500 (■), 1000 (▲), 2000 (◇), and 5000 (□) μM. The concentration of ATP was 500 μM in each assay. (C) ASP was varied from 250 to 5000 μM at fixed ATP concentrations of 15 (◆), 30 (▲), 60 (■), 120 (Δ), and 300 (□) μM. The concentration of CAIR was 20 μM in each assay.

of substrate. Mg^{2+}, Mn^{2+}, and Ca^{2+} are all activators of AMPSase. Ca^{2+}-activated AMPSase displayed a maximum rate of 15% relative to the Mg^{2+}-catalyzed reaction, but the K_m for ASP is severalfold lower in Ca^{2+}-catalyzed than in Mg^{2+}-catalyzed reactions (*30*).

A plot of initial velocity against Mg^{2+} concentration at fixed levels of ATP, CAIR, and ASP indicates a metal concentration in excess of that necessary to put all of the ATP into a $MgATP^{2-}$ complex [formation constant of 73000 M^{-1} at pH 7.8 (*31*)]. SAICAR synthetase either requires a metal ion in addition to that associated with ATP or uses ATP in a conformation that lowers its affinity for Mg^{2+} relative to that of the free nucleotide. Similar observations have been made regarding the Mg^{2+} concentration for optimal AMPSase activity (*30*).

Effect of pH on the SAICAR Synthetase Reaction. SAICAR synthetase at saturating levels of substrates exhibits optimal activity at pH 7.8 (data not shown). Over the pH range 7−8, the coupling system retained its ability to monitor ADP production from ATP.

Scheme 1

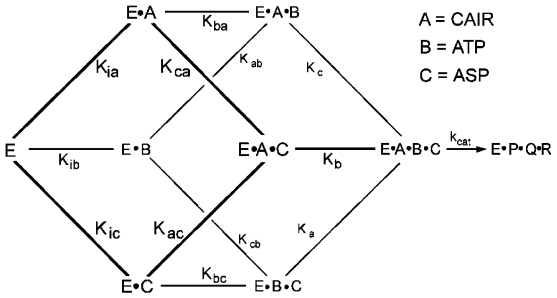

Kinetic Mechanism. Initial rate kinetic data were collected, holding one substrate at a saturating level while varying the concentrations of the other two substrates systematically relative to their respective K_m values. Double reciprocal plots of initial velocity for 75 distinct conditions of assay (Figure 1) appear as families of intersecting lines. The convergence of lines in each of the plots of Figure 1 excludes a number of mechanisms. Ping-pong mechanisms in which one or two of the three substrates bind (randomly or ordered) and lead to a product that dissociates from the enzyme before the addition of the third substrate will exhibit at least one plot with a family of parallel lines. Even the steady-state rate equation for the ordered ter-ter mechanism requires one plot in Figure 1 to be a family of parallel lines. All of the plots in Figure 1, however, reveal families of lines that intersect in the third quadrant, a result consistent with only a sequential kinetic mechanism. Fits of ping-pong, ordered, or partially ordered rapid equilibrium models provide decidedly inferior results and, in some cases, negative values for at least one parameter. The data of Figure 1, however, are consistent with the rate equation derived for the rapid equilibrium random sequential mechanism (Scheme 1):

$$V_{max}/v = 1 + K_a/A + K_b/B + K_c/C + K_aK_{bc}/AB + K_cK_{ab}/AC + K_bK_{ca}/BC + K_aK_{bc}K_{ic}/ABC \quad (1)$$

In the above, V_{max} is the maximum velocity, K_a, K_b, K_c, K_{bc}, K_{ab}, K_{ca}, and K_{ic} are dissociation constants, defined explicitly by reference to Scheme 1 and Table 1, and *A*, *B*, and *C* represent concentrations of CAIR, ATP, and ASP, respectively.

Data for each of the panels in Figure 1 were acquired on separate days. Hence systematic errors, in particular variations in V_{max}, are a concern in dealing with the analysis of data from Figure 1. Equation 1, however, requires that all data be consistent with a single value for V_{max}. Limiting forms of eq 1, which assume one substrate at a saturating concentration, allow different values for V_{max} for each panel of data in Figure 1:

$$V_{max}/v = 1 + K_a/A + K_b/B + K_aK_{bc}/AB \quad (2a)$$

$$V_{max}/v = 1 + K_a/A + K_c/C + K_cK_{ab}/AC \quad (2b)$$

$$V_{max}/v = 1 + K_b/B + K_c/C + K_bK_{ca}/BC \quad (2c)$$

Goodness of fit values between calculated data (from eqs 2a−c) and observed data (Figure 1) were below 4%. Equations 2a−c provide two independent determinations of

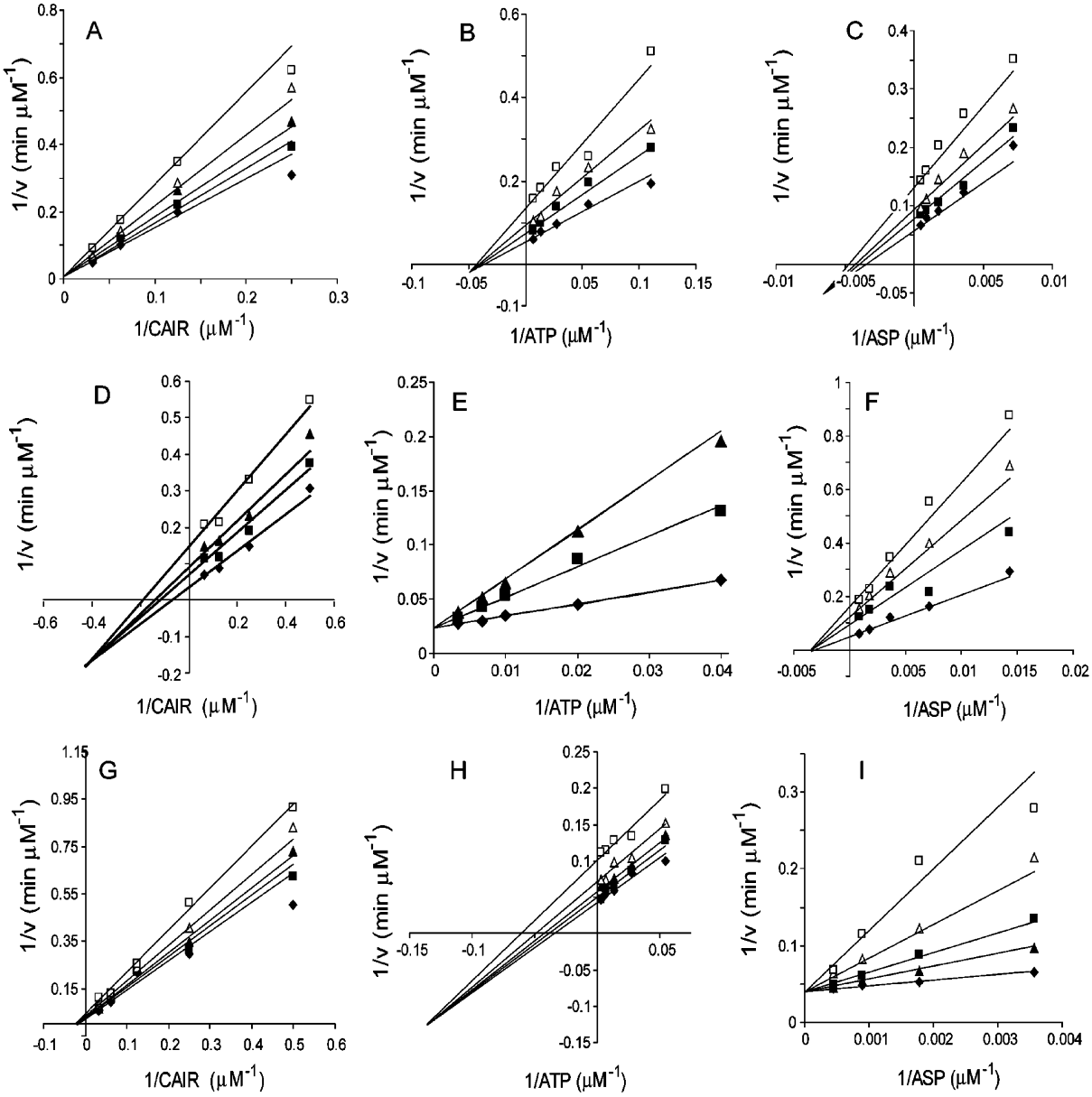

FIGURE 2: Plots of reciprocal velocity versus reciprocal substrate concentration at different concentrations of inhibitor. Mg^{2+} and ATP were added in a 1:1 ratio. The buffer conditions were 50 mM Hepes, 20 mM KCl, 6 mM $MgCl_2$, 0.2 mM NADH, 2 mM PEP, 10 units of pyruvate kinase, and 5 units of lactate dehydrogenase, pH 7.8. Lines come from eqs 4a−c using the parameters in Table 2. (A) ATP and ASP were held constant at 72.6 μM and 2.24 mM, respectively. The inhibitor (IMP) levels were 0 (◆), 1 (■), 2 (▲), 4 (Δ), and 8 (□) mM. (B) CAIR and ASP were held constant at 16 μM and 2.24 mM, respectively. The inhibitor (IMP) levels were 0 (◆), 2.5 (■), 5 (Δ), and 10 (□) mM. (C) ATP and CAIR were held constant at 72.6 and 16 μM, respectively. The inhibitor (IMP) concentrations were 0 (◆), 2.5 (■), 4.5 (Δ), and 9 (□) mM. (D) ATP and ASP were held constant at 72.6 μM and 2.24 mM, respectively. The inhibitor (AMP-PNP) concentrations were 0 (◆), 0.6 (■), 1 (▲), and 2 (□) mM. (E) CAIR and ASP were held constant at 16 μM and 2.24 mM, respectively. The inhibitor (AMP-PNP) concentrations were 0 (◆), 0.4 (■), and 0.8 (▲) mM. (F) ATP and CAIR were held constant at 72.6 and 16 μM, respectively. The inhibitor (AMP-PNP) concentrations were 0 (◆), 0.6 (■), 1 (Δ), and 1.5 (□) mM. (G) ATP and ASP were held constant at 72.6 μM and 2.24 mM, respectively. The inhibitor (maleate) concentrations were 0 (◆), 2 (■), 4 (▲), 8 (Δ), and 16 (□) mM. (H) CAIR and ASP were held constant at 16 μM and 2.24 mM, respectively. The inhibitor (maleate) concentrations were 0 (◆), 2 (■), 4 (▲), 8 (Δ), and 16 (□) mM. (I) ATP and CAIR were held constant at 72.6 and 16 μM, respectively. The inhibitor (maleate) concentrations were 0 (◆), 2 (▲), 4 (■), 8 (Δ), and 16 (□) mM.

the dissociation constants K_a, K_b, and K_c and three independent determinations of V_{max}. These independent determinations are in reasonable agreement (Table 1). Values for V_{max} (in units of nanomoles of product per minute) are 40 ± 3, 37 ± 2, and 35 ± 2 from eqs 2a−c and Figure 1, respectively. Values for dissociation constants, not explicitly represented in eqs 2a−c, were determined from relationships listed in Table 1.

Segel (*32*) defines a set of interaction parameters, α, β, and γ, which provide measures of binding antagonism/synergism between substrates B and C, A and C, and A and B, respectively. Values for interaction parameters between 0 and 1 reflect binding synergism, whereas numbers greater than unity indicate binding antagonism. The interaction parameters α, β, and γ are ratios of equilibrium constants indicated in Table 1.

Steady-state ordered and rapid equilibrium random mechanisms for two substrate systems are indistinguishable by data such as those in Figure 1. Rate equations derived by the assumption of steady-state kinetics for three-substrate systems are far more complex than for two substrate systems, and it is not clear in practice whether the data of Figure 1 can exclude all possible steady-state ordered mechanisms for three substrates. As a means of verifying the rapid equilibrium random mechanism for SAICAR synthetase, data were obtained in the presence of dead-end competitive inhibitors for ATP, CAIR, and ASP, using protocols developed by Fromm (*33*). Finding a set of appropriate competitive inhibitors, however, proved challenging. AMP-PNP was satisfactory as a competitive inhibitor with respect to ATP (Figure 2E). 5-Aminoimidazole ribonucleotide (AIR) exhibited potent inhibition of SAICAR synthetase, but its chemical instablity resulted in data of unsatisfactory quality. Instead, inhibition by IMP was reproducible and competitive with respect to CAIR (Figure 2A). Succinate, fumarate, and malate did not inhibit SAICAR synthetase at concentrations as high as 30 mM, and hadacidin caused only 50% inhibition at concentrations of 30 mM. Inhibition by maleate, however, was reasonably potent and competitive with respect to ASP (Figure 2I).

In the analysis of data in Figure 2, if an inhibitor I competes with A, then the following equilibria hold:

$$\mathrm{E} + \mathrm{I} = \mathrm{EI},\ K_1$$

$$\mathrm{EI} + \mathrm{B} = \mathrm{EIB},\ K_2$$

$$\mathrm{EIB} + \mathrm{C} = \mathrm{EIBC},\ K_3$$

$$\mathrm{EI} + \mathrm{C} = \mathrm{EIC},\ K_4$$

$$\mathrm{EIC} + \mathrm{B} = \mathrm{EIBC},\ K_5$$

$$\mathrm{EB} + \mathrm{I} = \mathrm{EIB},\ K_6$$

$$\mathrm{EIB} + \mathrm{C} = \mathrm{EIBC},\ K_7$$

$$\mathrm{EC} + \mathrm{I} = \mathrm{EIC},\ K_8$$

$$\mathrm{EBC} + \mathrm{I} = \mathrm{EIBC},\ K_9$$

The rate equation (eq 3) for such is

$$E_0/v = \Phi_0 + (\Phi_1/A)(1 + I/K_9) + \Phi_2/B + \Phi_3/C + (\Phi_4/AC)(1 + I/K_3) + (\Phi_5/AB)(1 + I/K_6) + \Phi_6/BC + (\Phi_7/ABC)(1 + I/K_1) \quad (3)$$

E_0 is the total concentration of enzyme, and parameters Φ_{0-7}, in Dalziel notation (*34*), are combinations of equilibrium constants defined in Scheme 1. The exact definitions of Φ_{0-7}, however, have no bearing on our analysis here. Under the conditions of assay, concentrations of two of three substrates are fixed at twice their values of K_m. By fixing the concentration of two substrates, for instance, B and C, eq 3 reduces to the mathematical form of linear competitive inhibition for a single substrate system:

$$E_0/v = K' + K_a'/A + K_a'/K_{is}'(I/A) \quad (4a)$$

Table 2: Mechanisms of Inhibition for Specific Substrate−Inhibitor Combinations[a]

	inhibitor		
substrate	AMP-PNP	IMP	maleate
ATP	competitive $K_{is}' = 0.26 \pm 0.02$	noncompetitive $K_{is}' = 7 \pm 1$ $K_{ii}' = 9 \pm 2$	noncompetitive $K_{is}' = 12 \pm 1$ $K_{ii}' = 50 \pm 30$
CAIR	noncompetitive $K_{is}' = 0.6 \pm 0.2$ $K_{ii}' = 4 \pm 2$	competitive $K_{is}' = 9.1 \pm 0.4$	noncompetitive $K_{is}' = 15 \pm 9$ $K_{ii}' = 40 \pm 10$
ASP	noncompetitive $K_{is}' = 0.7 \pm 0.1$ $K_{ii}' = 0.6 \pm 0.1$	noncompetitive $K_{is}' = 7 \pm 1$ $K_{ii}' = 13 \pm 6$	competitive $K_{is}' = 16 \pm 3$

[a] Details of the conditions of assay are given in the legend to Figure 2. K_{is}' is the apparent inhibition constant determined from the slope of the rate equation, and K_{ii}' is the apparent inhibition constant determined from the intercept of the rate equation. Inhibition constants are in units of mM.

By fixing concentrations of A and B and of A and C, eq 3 simplifies to eq 4b and eq 4c, respectively, both similar in form to linear noncompetitive inhibition for a single substrate system:

$$E_0/v = K' + I/K_{ii}' + K_c'/C + K_c'/K_{is}'(I/C) \quad (4b)$$

$$E_0/v = K' + I/K_{ii}' + K_b'/B + K_b'/K_{is}'(I/B) \quad (4c)$$

Hence, of the three plots for a specific inhibitor, one is competitive, but the other two are noncompetitive. Due to the symmetery of the random mechanism, inhibitors competitive with respect to B and C will result in analogous patterns of inhibition, i.e., a competetive inhibitor for B will exhibit noncompetitive inhibition patterns with respect to substrates A and C, and a competitive inhibitor for C will exhibit noncompetitive inhibition patterns with respect to substrates A and B. The inhibition patterns illustrated in Table 2 are unique to the rapid equilibrium random ter-ter mechanism.

The protocol used here does not provide numerical values for the constants of inhibition K_{1-9}. K', K_a', K_b', K_c', K_{is}', and K_{ii}' in eqs 4a−c are related to Φ_{0-7}, K_{1-9}, and A, B, and C by relatively complex relationships. In eq 4a, for instance, $K_a'/K_{is}' = \Phi_1/K_9 + \Phi_4/(CK_8) + \Phi_5/(BK_6) + \Phi_7/(BCK_1)$. Hence, the constants reported in Table 2 are apparent values. K_{ii}' is the apparent inhibition constant derived from the change in the intercept with increasing inhibitor concentration for a noncompetitive model, and K_{is}' is the apparent inhibition constant derived from the change in slope with increasing inhibitor concentration of a noncompetitive or competitive model. The analysis here rigorously establishes whether the mechanism of inhibition is competitive or noncompetitive, thereby determining the mechanism of SAICAR synthetase.

DISCUSSION

An examination of the literature reveals that very little information is available on the mechanism of action of SAICAR synthetase. Because of our long interest in AMPSase, dating from 1958 (*4*), and the obvious similarity between the substrate specificities of the two enzymes, we chose to investigate SAICAR synthetase in detail.

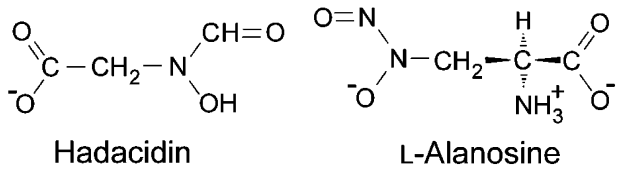

FIGURE 3: Chemical structures of hadacidin and L-alanosine.

The kinetic mechanism of SAICAR synthetase is sequential with the random addition of substrates. The observed mechanism is the same as that determined for *E. coli* AMPSase by comparable methods (*18*). Even though the two enzymes have a common kinetic mechanism, significant differences are evident. Data from equilibrium isotope exchange kinetics and electron paramagnetic resonance indicate strong synergism in the binding of IMP and GTP in bacterial and mammalian AMPSases (*19*, *36*). The synergism probably reflects the formation of 6-phosphoryl-IMP, a reaction that occurs in the active site of AMPSase in the absence of ASP (*36*−*38*). In contrast, the interaction parameters (α, β, and γ) from the fit of eq 1 are positive, indicating the presence of substrate binding antagonism for SAICAR synthetase. The data here offer no evidence for a tightly bound phosphoryl intermediate but cannot exclude the formation of such an intermediate.

The K_{ia} value in Table 1 infers a tight interaction between CAIR and the free enzyme, but under in vivo conditions ATP and ASP may always saturate the active site as there is lesser binding antagonism between these substrates ($\alpha = 3.9$) than for ATP and CAIR ($\gamma = 15$) and ASP and CAIR ($\beta = 11$). Hence, the Michaelis constant K_a, some 100-fold higher than K_{ia}, may better represent the in vivo binding affinity of CAIR to SAICAR synthetase. If antagonism between CAIR and ATP is due to steric interactions involving the γ-phosphoryl group, then ADP could be a potent feedback inhibitor of SAICAR synthetase. Maintaining the enzyme as a ternary E·ATP·ASP complex in vivo may be the strategy by which SAICAR synthetase avoids feedback inhibition not only by ADP but by SAICAR as well.

Succinate, L-malate, and fumarate, Krebs cycle intermediates, are present in *E. coli* at total concentrations (ap-

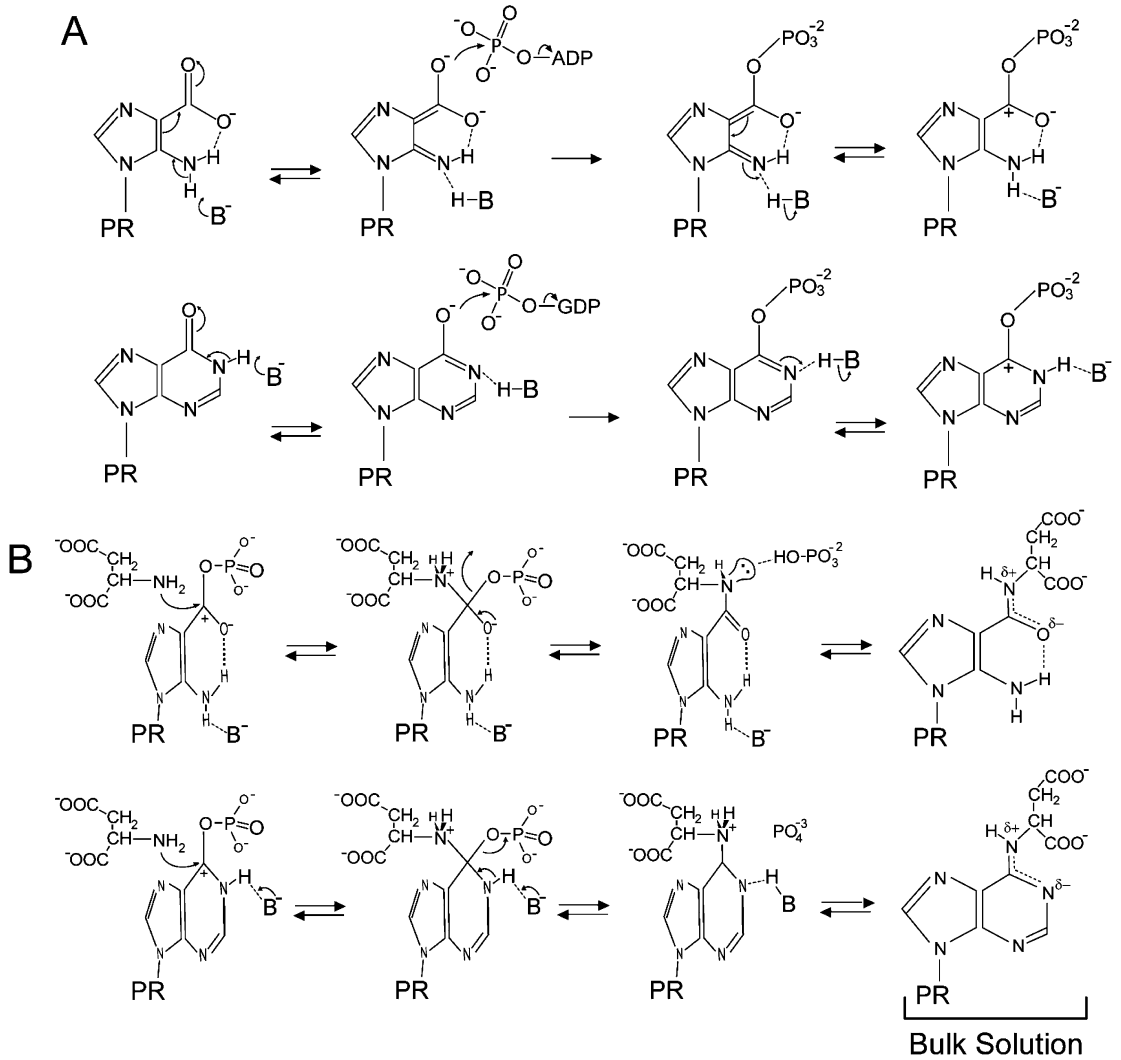

FIGURE 4: Parallels between proposed chemical mechanisms of AMPSase and SAICAR synthetase. (A) A putative catalytic base abstracts a proton from the 5-amino group of CAIR in SAICAR synthetase, enhancing the nucleophilic properties of the oxygen that attacks the γ-phosphoryl group of ATP (top). The catalytic base, Asp13 in *E. coli* AMPSase, abstracts the proton from the N-1 position of IMP, generating the 6-oxyanion that attacks the γ-phosphoryl group of GTP (bottom). Reprotonation of atom N-5 of CAIR (top) and atom N-1 of IMP (bottom) localizes positive charge on C-4 of CAIR and C-6 of IMP, respectively. (B) Nucleophilic attack by the α-amino group of ASP results in tetrahedral transition states (SAICAR synthetase, top; AMPsase, bottom) and the formation of product bound to the active site in a high-energy conformation. Products relax into minimum energy conformers in the bulk solution.

proximately 1 mM) comparable to that of ASP (*39*). Evidently, both AMPSase and SAICAR synthetase have evolved mechanisms which favor the selection of ASP over other relatively abundant dicarboxylic acids, as neither succinate, L-malate, nor fumarate inhibit SAICAR synthetase at concentrations of up to 30 mM, and of the above, only succinate is a weak inhibitor of AMPSase ($K_i \sim 1$ mM) (*5*). L-Malate, a putative substrate of yeast SAICAR synthetase (*10*), is not a substrate for the *E. coli* enzyme.

By definition, the substrate and inhibitor in competitive inhibition need only be mutually exclusive in their binding; however, if the substrate and inhibitor are similar in structure, it is reasonable to assume that both ligands compete for the active site. Inhibition of SAICAR synthetase by maleate, a property shared by AMPSase (*5*), infers a *cis*-like conformation for ASP in its enzyme-bound state. Indeed, the succinyl moiety of adenylosuccinate adopts such a conformation in its crystallographic complexes with AMPSase (*20*). The requirement for a *cis*-like conformer presumably allows AMPSase and SAICAR synthetase to discriminate against fumarate.

The mechanism by which SAICAR synthetase avoids inhibition by succinate and malate suggests a critical role for the α-amino group in the recognition of ASP. The large value for the interaction parameter β (Table 1), for instance, infers significant binding antagonism between ASP and CAIR. The most probable source of that antagonism is a steric clash between the α-amino group of ASP and the carbon atom of the 4-carboxyl group of CAIR. Succinate would avoid that steric clash and, as a consequence, should bind to the active site with higher affinity than ASP. Yet, succinate is not an inhibitor of SAICAR synthetase. This "succinate paradox" can be explained if the recognition of the α-amino group of ASP is a prerequisite for the binding of its carboxyl groups. The absence of malate inhibition further suggests an absolute need for two hydrogen bonds involving the α-amino group, both of which are proton donors to the protein.

The lack of inhibition of SAICAR synthetase by hadacidin (Figure 3) further underscores a fundamental difference in the recognition of ASP by SAICAR synthetase and AMPSase. For the latter enzyme, hadacidin is a potent inhibitor ($K_i \sim 10^{-6}$ M), competitive with respect to ASP (*40*−*42*). The *N*-formyl group of hadacidin coordinates the active site Mg^{2+} in AMPSase, while its *N*-hydroxyl group hydrogen bonds with an essential aspartyl side chain (*12*, *36*−*38*). The *N*-formyl and *N*-hydroxyl groups of hadacidin together may support a more stable set of interactions than does the α-carboxyl group of ASP (*3*). Hadacidin, however, does not have a functional group analogous to the α-amino group of ASP and, consistent with the hypothesis above, does not bind with high affinity to SAICAR synthetase. L-Alanosine, on the other hand, retains the α-amino group and supports SAICAR synthetase activity with a K_m nearly equal to that of ASP.

As CAIR competes with IMP for the active site of SAICAR synthetase, its 4-carboxyl and the 5-amino groups may form an intramolecular hydrogen bond and mimic the 6-atom ring of a purine nucleotide. Recognition of CAIR as a pseudopurine nucleotide suggests parallels between the chemical mechanism of AMPsase, well established by investigation (*7*, *12*, *15*, *36*−*38*), and that of SAICAR synthetase (Figure 4). Proton abstraction by a catalytic base, phosphorylation of the resulting oxyanion, reprotonation of the phosphoryl intermediate to generate a carbocation, and the nucleophilic addition of ASP represent plausible steps in the chemical mechanisms of both enzymes.

Regardless of similarities in the kinetic mechanisms of SAICAR synthetase and adenylosuccinate synthetase established here, and the suggested similarities in chemical mechanism, these two enzymes seem to have evolved different strategies for the recognition of a common substrate (ASP) and the extent to which they stabilize their respective carbonyl phosphate intermediates. Structural investigations should more precisely define protein−ligand interactions and provide the basis for experiments to test putative similarities in the chemical mechanisms of SAICAR synthetase and AMPSase.

ACKNOWLEDGMENT

This paper is dedicated to the memory of Frederick B. Rudolph (1944−2003), who helped to formulate many of the kinetic protocols used in this study.

REFERENCES

1. Lukens, L. N., and Buchanan, J. M. (1959) Biosynthesis of the purines XXIII: the enzymatic synthesis of *N*-(5-amino-1-ribosyl-4-imidazolylcarbonyl)-L-aspartic acid 5′-phosphate, *J. Biol. Chem. 234*, 1791−1798.
2. Miller, R. W., and Buchanan, J. M. (1962) Biosynthesis of the purines XXVII: *N*-(5-amino-1-ribosyl-4-imidazolylcarbonyl)-L-aspartic acid 5′-phosphate kinosynthetase, *J. Biol. Chem. 237*, 485−490.
3. Meyer, E., Leonard, N. J., Bhat, B., Stubbe, J., and Smith, J. M. (1992) Identification and characterization of *pur*E, *pur*K, and *pur*C gene products: identification of a previously unrecognized energy requirement in the purine biosynthetic pathway, *Biochemistry 31*, 5022−5032.
4. Fromm, H. J. (1958) On the equilibrium and mechanism of adenylosuccinate synthetase, *Biochim. Biophys. Acta 29*, 255−262.
5. Honzatko, R. B., Stayton, M. M., and Fromm, H. J. (1999) Adenylosuccinate synthetase: recent developments, *Adv. Enzymol. Relat. Areas Mol. Biol. 73*, 57−102.
6. Stayton, M. M., Rudolph, F. B., and Fromm, H. J. (1983) Regulation, genetics, and properties of adenylosuccinate synthetase: a review, *Curr. Top. Cell. Regul. 22*, 103−141.
7. Honzatko, R. B., and Fromm, H. J. (1999) Structure−function studies of adenylosuccinate synthetase from *Escherichia coli*, *Arch. Biochem. Biophys. 370*, 1−8.
8. Gale, G. R., and Smith, A. B. (1968) Alanosine and hadacidin—comparison of effects on adenylosuccinate synthetase, *Biochem. Pharmacol. 17*, 2495−2498.
9. Tyagi, A. K., and Cooney, D. A. (1980) Identification of the antimetabolite of L-alanosine, L-alanosyl-5-amino-4-imidazole-carboxylic acid ribonucleotide, in tumors and assessment of its inhibition of adenylosuccinate synthetase, *Cancer Res. 40*, 4390−4397.
10. Alenin, V. V., Ostanin, K. V., Kostikova, T. R., Domkin, V. D., Zubova, V. A., and Smirnov, M. N. (1992) Substrate specificity of phosphoribosyl-aminoimidazole-succinocarboxamide synthetase (SAICAR synthetase) from *Saccharomyces cerevisiae* yeast, *Biokhimiya 57*, 845−855.
11. Levdikov, V. M., Barynin, V. V., Grebenko, A. I., Melik-Adamyan, W. R., Lamzin, V. S., and Wilson, K. S. (1998) The structure of SAICAR synthetase: an enzyme in the *de novo* pathway of purine nucleotide biosynthesis, *Structure 6*, 363−376.
12. Poland, B. W., Fromm, H. J., and Honzatko, R. B. (1996) Crystal structure of adenylosuccinate synthetase from *Escherichia coli* complexed with GDP, IMP, hadacidin, NO_3^- and Mg^{2+}, *J. Mol. Biol. 264*, 1013−1027.

13. Wang, W., Gorrell, A., Honzatko, R. B., and Fromm, H. J. (1997) A study of *Escherichia coli* adenylosuccinate association states and the interface residues of the homodimer, *J. Biol. Chem. 272*, 7078−7084.
14. Borza, T., Iancu, C. V., Pike, E., Honzatko, R. B., and Fromm, H. J. (2003) Variation in the response of mouse isozymes of adenylosuccinate synthetase to inhibitors of physiological relevance, *J. Biol. Chem. 278*, 6673−6679.
15. Eaazhisai, K., Jayalakshmi, R., Gayathri, P., Anand, R. P., Sumathy, K., Balaram, H., and Murthy, M. R. (2004) Crystal structure of fully ligated adenylosuccinate synthetase from *Plasmodium falciparaum*, *J. Mol. Biol. 335*, 1251−1264.
16. Prade, L., Cowan-Jacob, S. W., Chemla, P., Potter, S., Ward, E., and Fonne-Pfister, R. (2000) Stuctures of adenylosuccinate synthetase from *Triticum aestivum* and *Arabidopsis thaliana*, *J. Mol. Biol. 296*, 569−577.
17. Batova, A., Diccianni, M. B., Omura-Minamisawa, M., Yu, J., Carrera, C. J., Bridgeman, L. J., Kung, F. H., Pullen, J., Amylon, M. D., and Yu, A. L. (1999) Use of alanosine as a methylthioadenosine phosphorylase-selective therapy for T-cell acute lymphoblastic leukemia *in vitro*, *Cancer Res. 59*, 1492−1497.
18. Rudolph, F. B., and Fromm, H. J. (1969) Initial rate studies of adenylosuccinate synthetase with product and competitive inhibitors, *J. Biol. Chem. 244*, 3832−3839.
19. Cooper, B. F., Fromm, H. J., and Rudolph, F. B. (1986) Isotope exchange at equilibrium studies with rat muscle adenylosuccinate synthetase, *Biochemistry 25*, 7323−7327.
20. Iancu, C. V., Borza, T., Fromm, H. J., and Honzatko, R. B. (2002) Feedback inhibition and product complexes of recombinant muscle adenylosuccinate synthetase, *J. Biol. Chem. 277*, 40536−40543.
21. Laemmli, U. K. (1970) Cleavage of structural proteins during the assembly of the head of bacteriophage T_4, *Nature 227*, 680−685.
22. Bradford, M. M. (1976) A rapid and sensitive method for the quantitation of microgram quantities of protein utilizing the principle of protein-dye binding, *Anal. Biochem. 72*, 248−254.
23. Srivastava, P. C., Mancuso, R. W., Rousseau, R. J., and Robins, R. K. (1974) Nucleoside peptides 6: synthesis of certain *N*-(5-amino-1-(beta-d-ribofuranosyl)imiadole 4-carboxyl) amino acids related to naturally occurring intermediates in the purine biosynthetic pathway, *J. Med. Chem. 17*, 1207−1211.
24. Yoshikawa, M., Kato, T., and Takenishi, T. (1967) A novel method for phosphorylation of nucleosides to 5′-nucleotides, *Tetrahedron Lett. 50*, 5065−5068.
25. Drueckes, P., Schinzel, R., and Palm, D. (1995) Photometric microtiter assay of inorganic phosphate in the presence of acid-labile organic phosphates, *Anal. Biochem. 230*, 173−177.
26. Siano, D. B., Zyskind, J. W., and Fromm, H. J. (1975) A computer program for fitting and statistically analyzing initial rate data applied to bovine hexokinase type III isozyme, *Arch. Biochem. Biophys. 170*, 587−600.
27. Liu, F., and Fromm, H. J. (1990) Studies on the mechanism and regulation of rabbit liver fructose-1,6-bisphosphatase, *J. Biol. Chem. 265*, 7401−7406.
28. Merkler, D. J., and Schramm, V. L. (1987) A preparative method for the enzymatic 5′-monophosphorylation of nucleosides, *Anal. Biochem. 167*, 148−153.
29. Lukens, L. N., and Buchanan, J. M. (1959) Biosynthesis of purines XXIV: the enzymatic synthesis of 5-amino-1-ribosyl-4-imidazolecarboxylic acid 5′-phosphate from 5-amino-1-ribosylimidazole 5′-phosphate and carbon dioxide, *J. Biol. Chem. 234*, 1799−1805.
30. Kang, C., and Fromm, H. J. (1995) Identification of an essential second metal in the reaction mechanism of adenylosuccinate synthetase, *J. Biol. Chem. 270*, 15539−15544.
31. O'Sullivan, W. J., and Smithers, G. W. (1979) Stability constants for biologically important metal−ligand complexes, *Methods Enzymol. 63*, 294−336.
32. Segel, I. H., Ed. (1975) *Enzyme Kinetics, Behavior and Analysis of Rapid Equilibrium and Steady-state Enzyme Systems*, John Wiley & Sons, New York.
33. Fromm, H. J. (1979) Use of competitive inhibitors to study substrate binding order, *Methods Enzymol. 63*, 467−486.
34. Dalziel, K. (1957) Initial steady-state velocities in the evaluation of enzyme coenzyme substrate reaction mechanisms, *Acta Chem. Scand. 11*, 1706−1723.
35. Markham, G. D. (1977) Structure and function of enzymes, Ph.D. Thesis, University of Pennsylvania, Philadelphia, PA.
36. Poland, B. W., Bruns, C., Fromm, H. J., and Honzatko, R. B. (1997) Entrapment of 6-thiophosphoryl-IMP in the active site of crystalline adenylosuccinate synthetase from *Escherichia coli*, *J. Biol. Chem. 272*, 15200−15205.
37. Choe, J.-Y., Poland, B. W., Fromm, H. J., and Honzatko, R. B. (1999) Mechanistic implications from crystallographic complexes of wild-type and mutant adenylosuccinate synthetases from *Escherichia coli*, *Biochemistry 38*, 6953−6961.
38. Iancu, C. V., Borza, T., Fromm, H. J., and Honzatko, R. B. (2002) IMP, GTP, and 6-phosphoryl-IMP complexes of recombinant mouse muscle adenylosuccinate synthetase, *J. Biol. Chem. 277*, 26779−26787.
39. Gorrell, A., Wang, W., Underbakke, E., Hou, Z., Honzatko, R. B., and Fromm, H. J. (2002) Determinants of L-aspartate and IMP recognition in *Escherichia coli* adenylosuccinate synthetase, *J. Biol. Chem. 277*, 8817−8821.
40. Kackza, E. A., Gitterman, C. O., Dulaney, E. L., and Folkers, K. (1962) Hadacidin, a new growth-inhibitory substance in human tumor systems, *Biochemistry 1*, 340−343.
41. Shigeura, H. T., and Gordon, C. N. (1962) The mechanism of action of hadacidin, *J. Biol. Chem. 237*, 1937−1940.
42. Shigeura, H. T. (1967) Hadacidin, in *Antibiotics* (Gottlieb, D., and Shaw, P., Eds.) pp 451−456, Springer-Verlag, New York.

BI048191W